UMT-0207
PNL-4132
UC-70

Moisture Content Analysis of Covered Uranium Mill Tailings

D. W. Mayer
P. A. Beedlow
L. L. Cadwell

December 1981

Prepared for the U.S. Department of Energy
under Contract DE-AC06-76RLO 1830

Pacific Northwest Laboratory
Operated for the U.S. Department of Energy
by Battelle Memorial Institute

Battelle

PNL-4132

UMT-0207
PNL-4132
UC-70

MOISTURE CONTENT ANALYSIS OF COVERED URANIUM MILL TAILINGS

D. W. Mayer
P. A. Beedlow
L. L. Cadwell

December 1981

Prepared for
the U.S. Department of Energy
under Contract DE-AC06-76RLO 1830

Pacific Northwest Laboratory
Richland, Washington 99352

SUMMARY

The use of vegetation and rock covers to stabilize uranium mill tailings cover systems is being investigated by Pacific Northwest Laboratory. A modeling study of moisture movement through the tailings and cover layers was initiated to determine the effect of the stabilizing techniques.

The cover system was simulated under climatic conditions occurring at Grand Junction, Colorado. The cover consisted of a layer of wet clay/gravel mix followed by a capillary barrier of washed rock and a surface layer of fill soil. Vegetation and rock were used to stabilize the surface layer. The simulation yielded moisture content and moisture storage values for the tailings and cover system along with information about moisture losses due to evaporation, transpiration, and drainage.

The study demonstrates that different surface stabilization treatments lead to different degrees of moisture retention in the covered tailings pile. The evapotranspiration from vegetation can result in a relatively stable moisture content. Rock covers, however, may cause drainage to occur because they reduce evaporation and lead to a subsequent increase in moisture content. It is important to consider these effects when designing a surface stabilization treatment. Drainage may contribute to a groundwater pollution problem. A surface treatment that allows the cover system to dry out can increase the risk of atmospheric contamination through elevated radon emission rates.

CONTENTS

FIGURES

TABLES

INTRODUCTION

Uranium mill tailings consist of the waste or refuse left after uranium processing. The typical disposal method has been to slurry the tailings into large ponds that eventually dry out, leaving a tailings pile. Since the tailings contain significant quantities of radium, they emit radon gas, which is a decay product of radium. Because exposure to radon gas has been linked to lung cancer, concern has been expressed over the health and environmental aspects of open tailings piles. A number of sealant or barrier systems are being considered to contain radon and other toxic materials in inactive uranium mill tailings. To maintain long-term effectiveness, a sealant/barrier system must be protected from wind, water, ultraviolet radiation, frost, chemical reaction, and biological degradation.

Soil placed over a sealant/barrier system can provide a protective mantle if the soil is not lost by erosion. Vegetation is an attractive choice for controlling wind and water erosion since it is economical and self-renewing. In extremely arid regions, vegetation may not adequately stabilize the surface layer. In these areas rock covers may be required. However, by reducing evapotranspiration, rock covers may cause the moisture content of the tailings to increase.

Maintaining a high moisture content in covered uranium mill tailings helps reduce the surface emission of radon gas (Nelson et al. 1980, Mayer et al. 1981). Too high a moisture content, however, may result in drainage through the tailings pile and increase the potential for groundwater pollution. In response to these concerns, Pacific Northwest Laboratory (PNL)[a] contracted with the Department of Energy's Uranium Mill Tailings Remedial Action Program (UMTRAP), to develop a methodology for studying the effects of vegetated and rock covers on the moisture content in a covered uranium mill tailings system.

(a) Operated by Battelle Memorial Institute

This report introduces a methodology for analyzing the time varying moisture content in covered uranium mill tailings. A discussion is included on the application of the methodology to rock and vegetated cover systems under climatic conditions occurring at Grand Junction, Colorado. Comments are also included on how to improve the methodology to increase the accuracy of the moisture-content analysis.

CONCLUSIONS AND RECOMMENDATIONS

The results of this study indicate that care must be taken when selecting a surface stabilization system for a tailings pile. The moisture-content response of the tailings pile and cover system can be radically altered by different surface treatments. The two cases considered in this study indicate that (under climatic conditions occurring at Grand Junction, Colorado) the evapotranspiration from a vegetated cover can result in a relatively stable moisture content. A rock cover, however, may increase the moisture content of the tailings pile by significantly reducing evaporation. In fact, moisture storage may increase to the point that drainage occurs.

Future studies should refine the description of the surface boundary condition to provide a more accurate moisture sink term. This work should focus on better descriptions of plant growth and moisture extraction behavior as a function of climatological conditions. Additional work is required to more accurately describe the diffusion of water vapor through rock covers, and to quantify the effects of wind.

Once a cover system is selected, the modeling effort should also include an assessment of how the cover system affects radon gas emissions. This capability is already developed and can be directly coupled to the unsaturated flow analysis presented in this study (Nelson et al. 1980, Mayer et al. 1981). It is important to consider the effects of atmospheric contamination from uranium mill tailings, as well as the potential for groundwater contamination.

UNSATURATED FLOW CONSIDERATIONS

Uranium mill tailings usually occupy an unsaturated flow zone constituting the transition region between the atmosphere and a groundwater system. Unsaturated zone modeling has, therefore, been used for this study. An unsaturated flow zone gains moisture from precipitation, agricultural irrigation, and seepage from rivers and lakes. Moisture is lost by evaporation, plant transpiration, and drainage. Soil moisture moves in an unsaturated zone under the influences of gravity, Darcian flow, and vapor diffusion.

This chapter describes the processes that control moisture gain, loss, and movement in an unsaturated zone. Gravity causes downward movement of soil water until the restraining force due to capillary hydraulic potential (matric potential) is in balance with the gravity force. If the capillary action is stronger than the gravity force, upward moisture movement may occur. The movement by capillary action is called Darcian flow and is described by the hydraulic conductivity and the matric potential gradient, both of which are strongly dependent on the moisture content.

Movement of soil moisture by vapor diffusion is significant near the soil surface and is the primary mechanism controlling moisture loss by surface evaporation. Potential evaporation rates are the highest when the soil near the surface is nearly saturated; otherwise, a dry layer of soil limits evaporation. Moisture is also lost by plant transpiration. To model this mechanism, the relationship between the potential transpiration and the climatic conditions must be specified. Root zone extraction behavior must also be described, since plant roots remove moisture at different rates at different depths.

If the water infiltrating the soil profile exceeds the capability of the soil to store moisture, drainage will occur. This drainage may enter the groundwater system, depending on the depth of the water table.

The presence of soil layers complicates unsaturated flow modeling. Clay, silt, sand, and gravel layers affect the movement of soil water differently. Certain layers rapidly transmit soil moisture, while others impede its movement.

The computer code, UNSAT (Gupta et al. 1978), has been developed to solve the one-dimensional unsaturated flow equation. The code accounts for the important factors influencing the unsaturated zone, namely,

- water infiltration from precipitation or irrigation
- evaporation
- transpiration
- runoff
- drainage.

A new version of UNSAT called UNSATV (developed by Simmons and Gee 1981) has been used for this study because it is capable of modeling the effects of water vapor diffusion. For a more detailed description of these codes and applications of the codes, the reader is referred to the reference reports.

MOISTURE CONTENT ANALYSIS

The following three sections discuss the various aspects of modeling vegetated and rock cover systems. The basic input data and model setup common to both simulations are discussed. This discussion is followed by analysis of soil moisture dynamics under vegetation and rock cover surface treatments.

MODEL SETUP

The multilayer cover system investigated is one of three being developed at the Grand Junction, Colorado site. This particular system was simulated because the water content in the seal affects its performance as a radon barrier. The initial conditions used for the unsaturated flow analysis (Table 1) represent near-equilibrium conditions below the clay/gravel layer to the 763-cm-deep water table. The moisture conditions above the clay/gravel layer are the result of repeated simulations using the recorded climatic conditions and could represent the initial conditions from a long-term climatic history. The clay/gravel layer's moisture content is initially at a nearly saturated state. Table 2 summarizes the layer characteristics used for this simulation. The soil water characteristics reported by Simmons and Gee (1981) for the Grand Junction clay, rock, and tailings layers have been used. The soil water characteristics for the A+ clay/gravel mix are represented by the curves shown in Figures 1a and 1b.

Climatic parameters were obtained from monthly summaries of local climatological data[a] for Grand Junction, Colorado. The data from the summaries for the years 1976 and 1979 were provided in the following units: hourly precipitation (inches); temperature (°F) in terms of daily maximum, minimum, average, and average dew point temperature; average wind speed (m.p.h.); percent of possible sunshine and sky cover in tenths; and maximum and minimum relative humidity. Hourly precipitation determined the water infiltration rate for the modeling. Other climatic parameters were used to estimate potential evapotranspiration on a daily basis.

(a) Published by the U.S. Department of Commerce, National Climatic Center, Asheville, North Carolina.

TABLE 1. Soil Profile Depth Nodes and Initial Conditions for Simulation of the 1979 Climate of Grand Junction, Colorado

Soil Layer	Depth (cm)	Suction Head (cm)	Water Content
Grand Junction Clay	0.0	1450.0	0.170
	2.5	3167.0	0.172
	5.0	1293.0	0.175
	7.5	1230.0	0.177
	10.0	1176.0	0.179
	15.0	1090.0	0.183
	20.0	1025.0	0.187
	25.0	975.0	0.190
	30.0	935.0	0.192
	35.0	902.0	0.195
	40.0	874.0	0.197
	50.0	830.0	0.200
	60.0	796.0	0.203
	70.0	768.0	0.206
	80.0	746.0	0.208
	99.0	709.0	0.212
Rock	100.0	709.0	0.008
	110.0	709.0	0.008
	120.0	709.0	0.008
	129.0	709.0	0.008
A+ Clay/Gravel Mix	130.0	600.0	0.259
	132.0	600.0	0.259
	135.0	600.0	0.259
	140.0	600.0	0.259
	142.0	600.0	0.259
	144.0	600.0	0.259
Medium Tailings	145.0	651.0	0.141
	150.0	646.0	0.141
	160.0	629.0	0.142
	180.0	612.0	0.144
	200.0	590.0	0.145
	250.0	524.0	0.150
	300.0	467.0	0.155
	400.0	365.0	0.167
	500.0	265.0	0.185
	600.0	165.0	0.214
	650.0	155.0	0.238
	700.0	65.0	0.278
	750.0	15.0	0.370
	755.0	10.0	0.384
	760.0	5.0	0.399
Water Table	763.0	2.0	0.408

TOTAL INITIAL MOISTURE STORAGE 145.859 cm

TABLE 2. Layer Characteristics

Layer	Thickness (cm)	Material	Porosity (cm^3/cm^3)	Bulk Density (g/cm^3)
4	100	Overburden (Grand Junction clay)	0.468	1.37
3	30	Rock	0.320	1.80
2	15	Clay/Gravel mix (A+)	0.270	1.97
1	618	Medium tailings	0.458	1.47

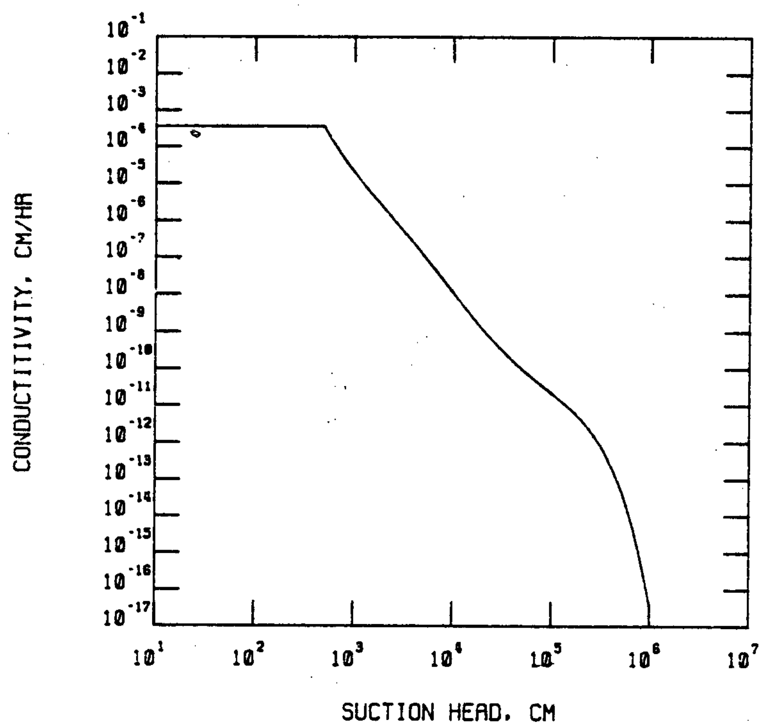

FIGURE 1a. Hydraulic Conductivity Versus Suction Head for Grand Junction A+ Clay/Gravel Mix

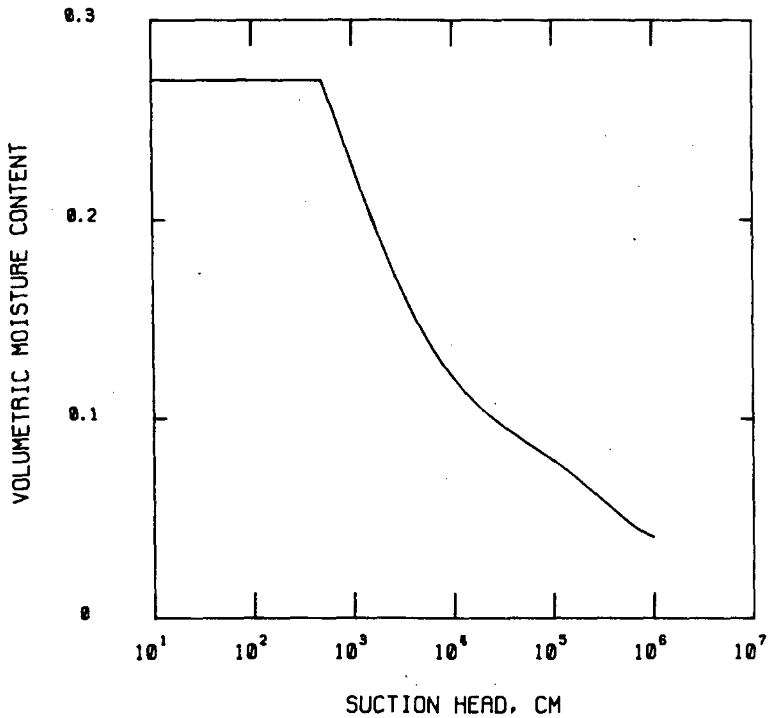

FIGURE 1b. Moisture Conductivity Versus Suction Head for Grand Junction A+ Clay/Gravel Mix

For both cover systems, UNSATV was run for one year using the climatic data for 1979 (wettest year on record). This simulation was started using the initial conditions shown in Table 1. The purpose of this one-year simulation was to allow the moisture content in the soil to adjust to the actual climate. Since this is simply an initialization procedure, the results for this year are not discussed here. The moisture content profile at the end of the one-year simulation was next used as the initial condition for a two-year simulation using repeated 1979 climate data and for a two-year simulation using repeated 1976 climate data (driest year on record). This approach provides two dry years and two wet years for comparison of the effects of climate on each surface treatment. The surface treatments can also be compared with each other and thereby illustrate the effects of vegetation and rock covers.

VEGETATED COVER SIMULATION

The purpose of this phase of the research effort is to examine how vegetation influences the moisture content of a covered uranium mill tailings pile. A plant community consisting of the following plant species (percentages are cover values) was modeled:

- 29% Artemisia tridentata (Big Sagebrush)
- 2% Atriplex confertifolia (Four-wing Saltbush)
- 2.5% Agropyron (Wheatgrass)
- 2.5% Bromus tectorum (Cheatgrass).

Thus, the plant community consisted of 36% plants and 64% bare soil.

Because UNSATV was originally developed for a single plant species, the above plant community was modeled as a single composite plant with the root density data and evapotranspiration (ET) data for each plant weighted appropriately. The data obtained for root density and ET for each plant are based on a plant community that would consist of reasonable amounts of bare soil. The composite plant characteristics are obtained by averaging the individual plant characteristics. The weighting factors for each plant are obtained by dividing the percent of plant cover for each species divided by the total percent of plant cover.

The root density must be specified so that the loss of moisture due to plant transpiration can be distributed appropriately throughout the root zones. The root densities for each plant were developed from data on root biomass and root weights reported in the literature (Branson et al. 1976, and Cline and Rickard 1974). The actual values are tabulated in the appendix. The two shrubs Artemisia tridentata and Atriplex confertifolia were assumed to have constant maximum root depths of 180 cm and 110 cm, respectively, and the perrenial grass was assumed to have a constant maximum root depth of 80 cm. The maximum root depth of the annual grass depends on the growing season as shown in Table 3. The two shrubs were assumed to have an active growing season starting on the 90th day of the year and ending on the 320th day of the year. The grasses were assumed to be actively growing from day 120 to day 190. It should be noted that the plant root model does not take into account the

TABLE 3. Growing Days Required for Annual Grass Roots to Reach Various Depths

Depth (cm)	Days	Depth (cm)	Days
0.0	5	30	20
2.5	6	35	25
5.0	7	40	35
7.5	8	50	40
10	10	60	50
15	11	70	60
20	15	80	70
25	16		

effects of climate or soil conditions on root growth. UNSATV is not currently able to account for these effects, although it would be possible to add this feature.

Modeling plant transpiration requires that the potential evapotranspiration (PET) be divided into its component parts: potential evaporation (PE) and potential transpiration (PT). Little information was available for describing this relationship for the shrubs, but information reported by Branson et al. (1970) indicates that the PT is approximately 85% of the PET. This relationship was assumed to hold for both shrubs throughout the growing season. A relationship that accounts for the variation of PT with growing season and PET has been discussed by Simmons and Gee (1981) for cheatgrass and has been used for both grasses.

Using this information, the simulations were performed as previously discussed. Figures 2a and 2b are plots of the moisture contents for selected days from the two wet years simulated. Figures 3a and 3b are for the two dry years simulated. An important feature to note is that, although the moisture content in the surface layer varies dramatically, the lower layers exhibit very little change in moisture content. By comparing Figure 2a with 3a and Figure 2b with 3b, we see that the dry climate results in a drying out of the upper layer and less variation of the moisture content throughout the year. Note that the moisture content in the upper layer is generally smaller and that the moisture content profiles do not change as much in Figures 3a and 3b.

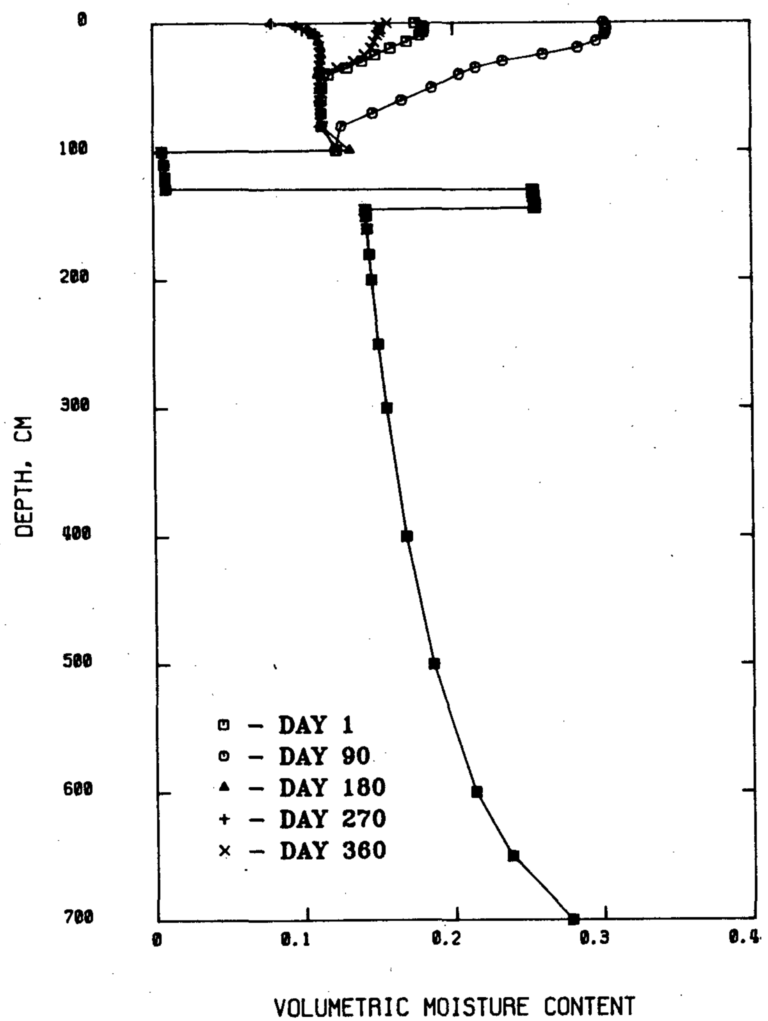

FIGURE 2a. Moisture Content Distribution for Vegetated Cover for Wet Year (1979) Climate Data--2nd Simulation Year

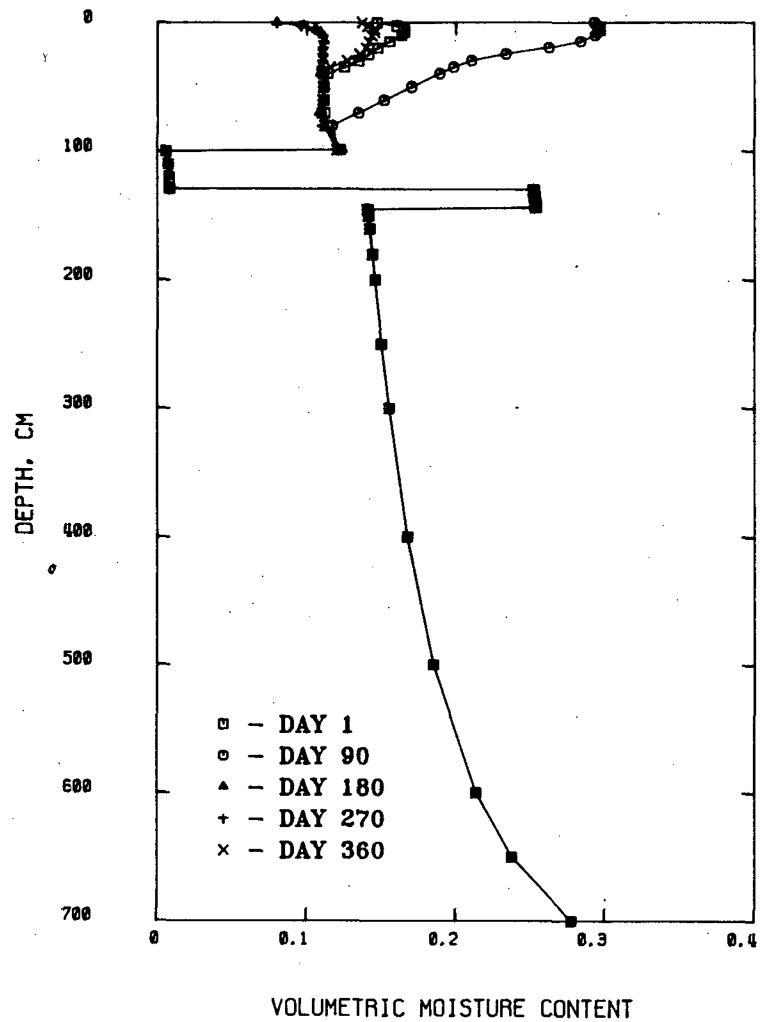

FIGURE 2b. Moisture Content Distribution for Vegetated Cover for Wet Year (1979) Climate Data--3rd Simulation Year

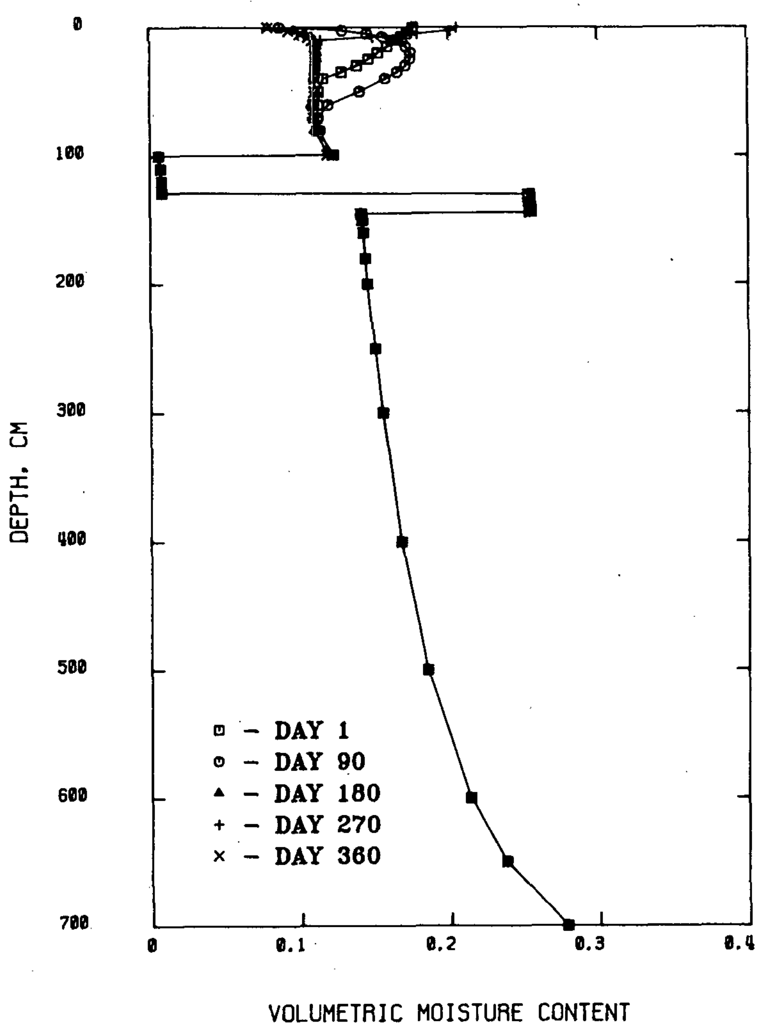

FIGURE 3a. Moisture Content Distribution for Vegetated Cover for Dry Year (1976) Climate Data--2nd Simulation Year

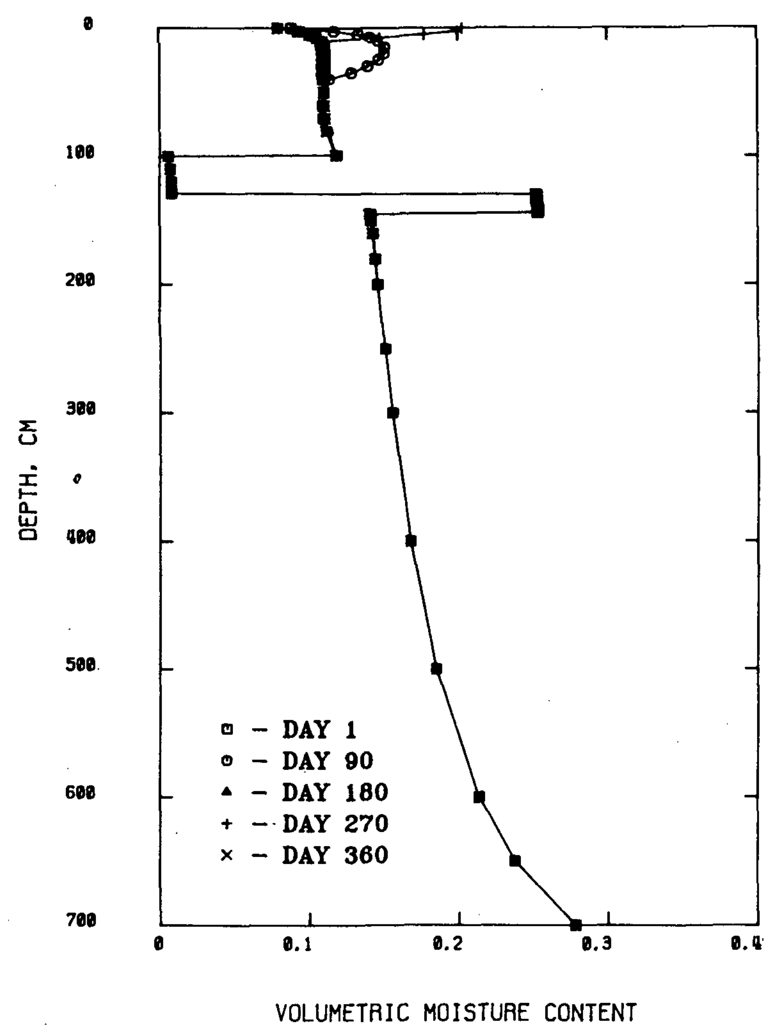

FIGURE 3b. Moisture Content Distribution for Vegetated Cover for Dry Year (1976) Climate Data--3rd Simulation Year

The moisture storage for the entire soil profile is plotted for the two wet years in Figures 4a and 4b and for the two dry years in Figures 5a and 5b. These plots illustrate the short-term variation in moisture storage due to rainfall events and seasonal variations. The moisture storage during the two wet years is nearly identical, although for the first five months of the second year, the soil profile is slightly drier. The soil profile for the two dry years is noticeably drier than during the two wet years. During the summer and early fall, however, the moisture storage for the wet years and for the dry years is identical.

The water balance for the wet years is summarized in Table 4; the dry years' water balance is summarized in Table 5. The initial storage values represent the amount of water stored in all four layers on day one for each year. The rainfall value is the amount of water from precipitation that is available for infiltration. The runoff values indicate the amount of precipitation that did not infiltrate but that flowed over the soil surface and eventually provided input to a stream or lake. The total amount of water lost by evaporation from the soil surface and the amount lost by transpiration are also given. The water that drains through the soil profile and out the bottom is listed. The final storage values indicate the amount of moisture stored in all four layers on the last day of each year. The mass balance error, a measure of the accuracy of the model results, is computed by comparing the difference in the change in water storage computed as the difference in initial and final water storage or by summing the rainfall, runoff, evaporation, transpiration, and drainage values (values must be added or subtracted as appropriate).

It is apparent from Table 4 that storage during the wet years has changed negligibly. Table 5 indicates that the two dry years result in a slight drying of the soil profile (approximately 2 cm of water). Note that no runoff or drainage occurred for either the wet or the dry years.

ROCK COVER SIMULATION

This phase of research examines the effect of rock on moisture storage in a covered uranium mill tailings. This analysis is essentially identical to

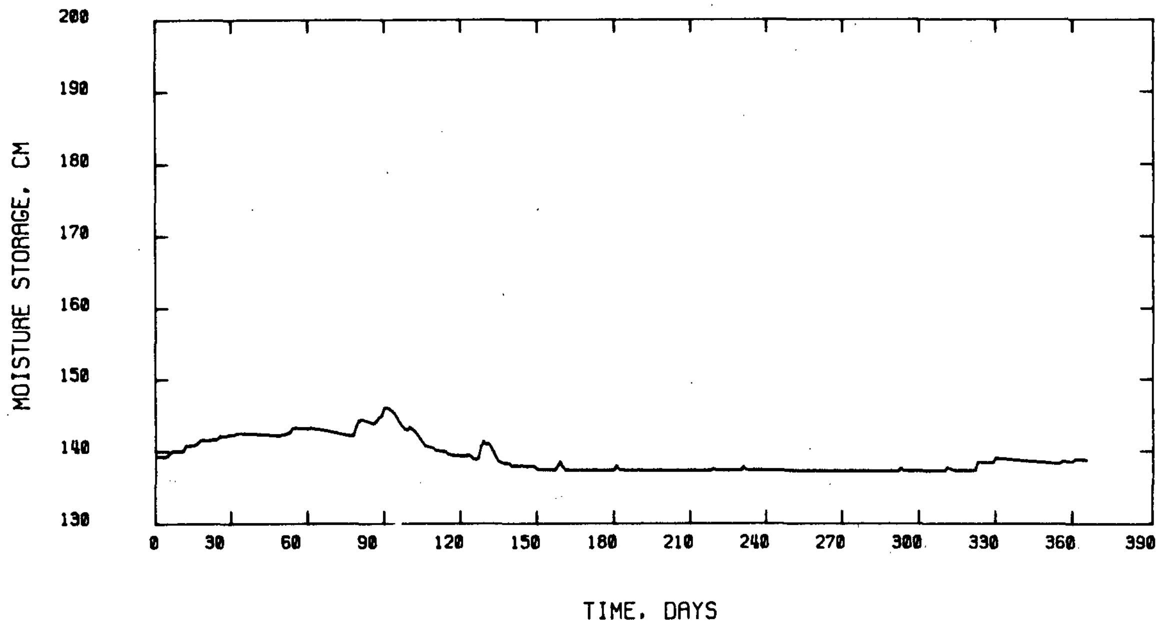

FIGURE 4a. Moisture Storage With Vegetated Cover for Wet Year (1979) Climate Data--2nd Simulation Year

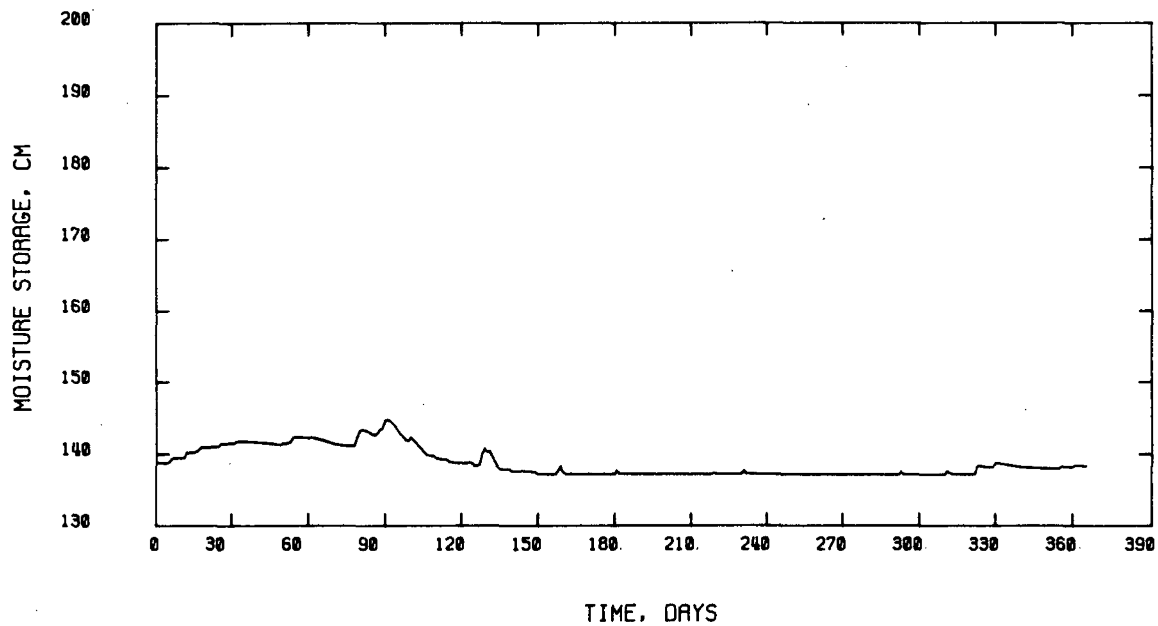

FIGURE 4b. Moisture Storage With Vegetated Cover for Wet Year (1979) Climate Data--3rd Simulation Year

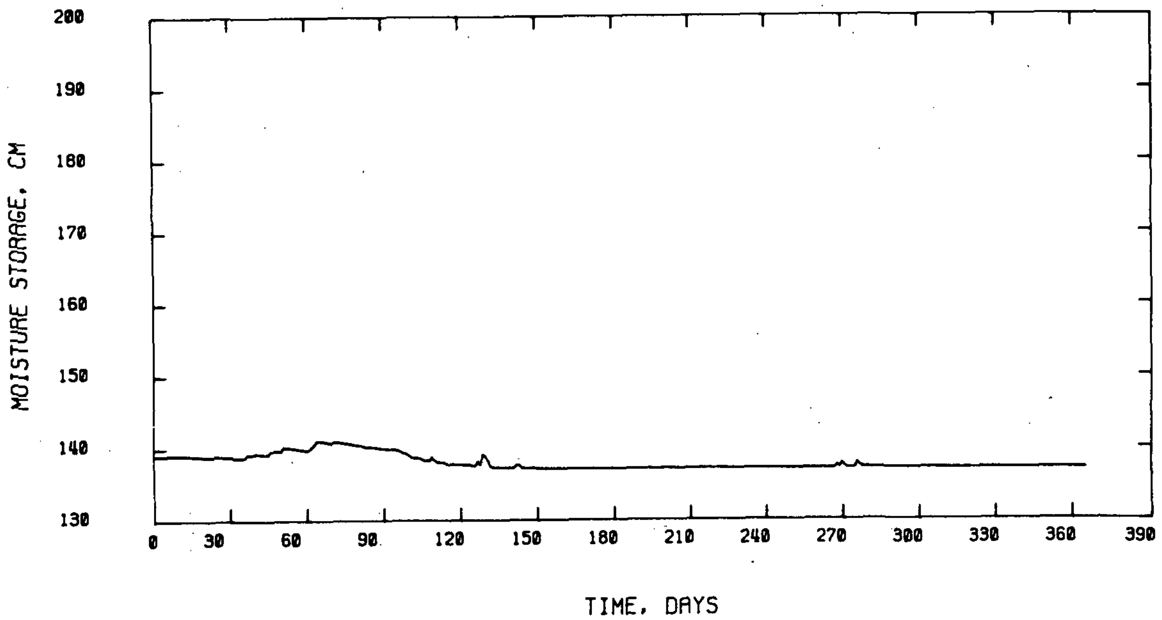

FIGURE 5a. Moisture Storage With Vegetated Cover for Dry Year (1976) Climate Data--2nd Simulation Year

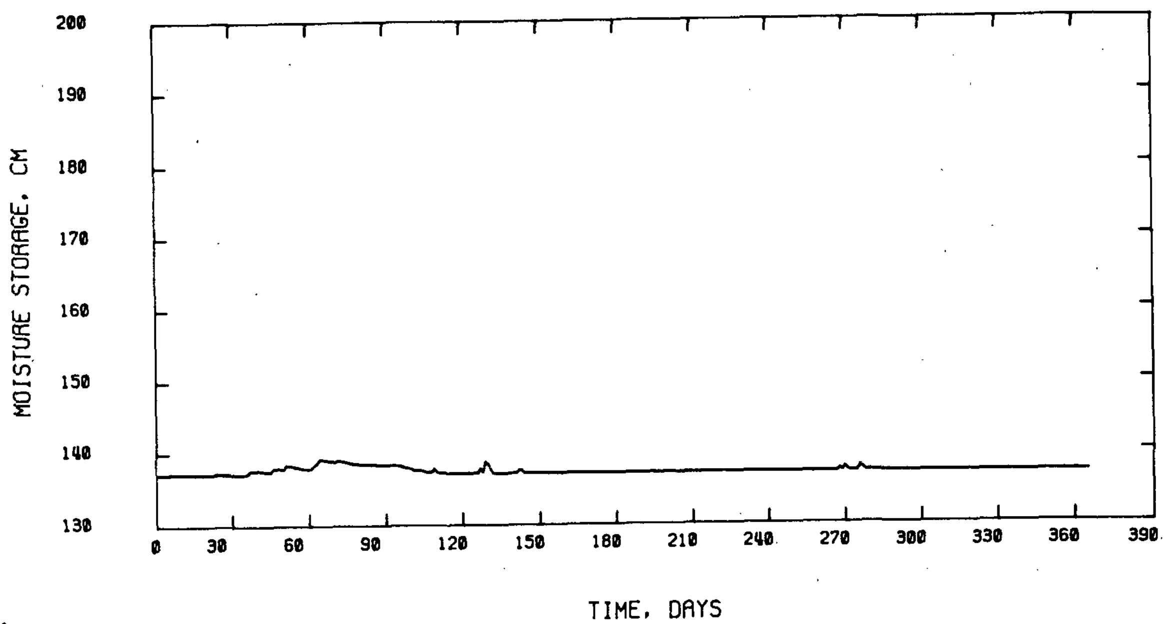

FIGURE 5b. Moisture Storage With Vegetated Cover for Dry Year (1976) Climate Data--3rd Simulation Year

TABLE 4. Water Balance for Two Wet Years, Vegetated Cover System

Water (cm)	Simulation Year 2	Simulation Year 3
Initial Storage	139.3	139.2
Rainfall	22.6	22.6
Runoff	0.0	0.0
Evaporation	5.8	5.8
Transpiration	16.2	16.3
Drainage	0.0	0.0
Final Storage	139.2	139.1
Mass Balance Error	0.6	0.6

TABLE 5. Water Balance for Two Dry Years, Vegetated Cover System

Water (cm)	Simulation Year 2	Simulation Year 3
Initial Storage	139.3	137.1
Rainfall	13.4	13.4
Runoff	0.0	0.0
Evaporation	6.0	5.1
Transpiration	8.8	7.5
Drainage	0.0	0.0
Final Storage	137.1	137.1
Mass Balance Error	0.8	0.9

the analysis for the vegetated cover except the plants have been removed, and 50 cm of rock (the same material used for layer 3, see Table 2) has been added to the top of the tailings pile.

Moisture will move through the rock primarily by a vapor diffusion process. UNSATV solves the unsaturated flow equation for liquid water movement and can simulate vapor diffusion through a thin mulch layer. To model the movement of water vapor through the relatively thick rock layer considered here, it is necessary to slightly modify UNSATV. This modification requires either the inclusion of a vapor diffusion model, or the liquid hydraulic conductivity for the rock layer can be increased to account for the additional moisture movement due to water vapor diffusion. The second method essentially models the vapor movement as liquid movement via the enhanced hydraulic conductivity. (This method is discussed in more detail by Simmons and Gee 1981).

Numerical difficulties may be experienced with the enhanced hydraulic conductivity approach when modeling vapor movement in rock covers. Since rock covers are typically very porous, wetting fronts due to precipitation will move through the rock relatively fast. This means that very small time steps will be required if large mass balance errors are to be avoided. In addition, soil water characteristics for the rock cover extending into the very dry region were not available. Therefore, evaporation through the rock cover has been modeled as a vapor diffusion process using the following equation:

$$E = D_a\,(P-\theta)\,\alpha\,(\rho_{air} - \rho_{soil})/\Delta Z$$

where,

D_a = water vapor diffusivity in air (typical value: 0.24 cm^2/sec)

P = material porosity on a volume basis

θ = moisture content on a volume basis

α = tortuosity (often assumed to be 0.5 for gravels)

ρ_{air} = water-vapor density in the air (typical units: g/cm^3)

ρ_{soil} = water-vapor density in the soil immediately below the rock (typical units: g/cm^3)

ΔZ = thickness of the rock layer (typical units: cm).

Note that this equation does not account for the influence of wind, which tends to increase the evaporation rate. The water-vapor densities in air and soil depend on the temperatures of the air and soil and are related to the respective vapor pressures by the ideal gas law. The vapor pressure at the soil surface (which is nearly saturated until the soil becomes very dry) is calculated from the water-vapor-adsorption-isotherm equation proposed by Fink and Jackson (1973):

$$\ln \theta = A + B \ln [(RH)^{-C} - 1]$$

where,

A, B and C are empirically determined coefficients and
RH is the relative humidity.

Values of the coefficients for Grand Junction clay soil are A = -2.916, B = -0.185 and C = 1.49 (Simmons and Gee 1981).

Since the moisture movement in the rock layer is not directly modeled, it is necessary to assume a value for the moisture content, θ. For this study, it was assumed that the moisture from precipitation would move instantaneously to the soil surface; therefore, θ was taken to be zero. The material used for the surface rock layer was the same as the vapor barrier rock layer, so the porosity was fixed at 0.320.

The resulting moisture content profiles are shown in Figures 6a and 6b for the two wet years and in Figures 7a and 7b for the two dry years. Note that the rock cover is not shown on these plots, because the liquid water movement was not modeled for the rock cover. It is apparent from these plots that the rock cover has had a significant effect on the moisture content in the tailings pile in comparison to vegetation cover treatments. The moisture content in the soil layer is much higher, and the seasonal variation in moisture content is not as great (compare with Figures 2 and 3). The major difference, however, is that the tailings layer is becoming wetter, meaning that water is now draining from the upper layers. Note also that the moisture content throughout the tailings pile is now being affected by the climatic conditions (i.e., the moisture content is also changing in the vapor barrier rock, clay/gravel and tailings layers).

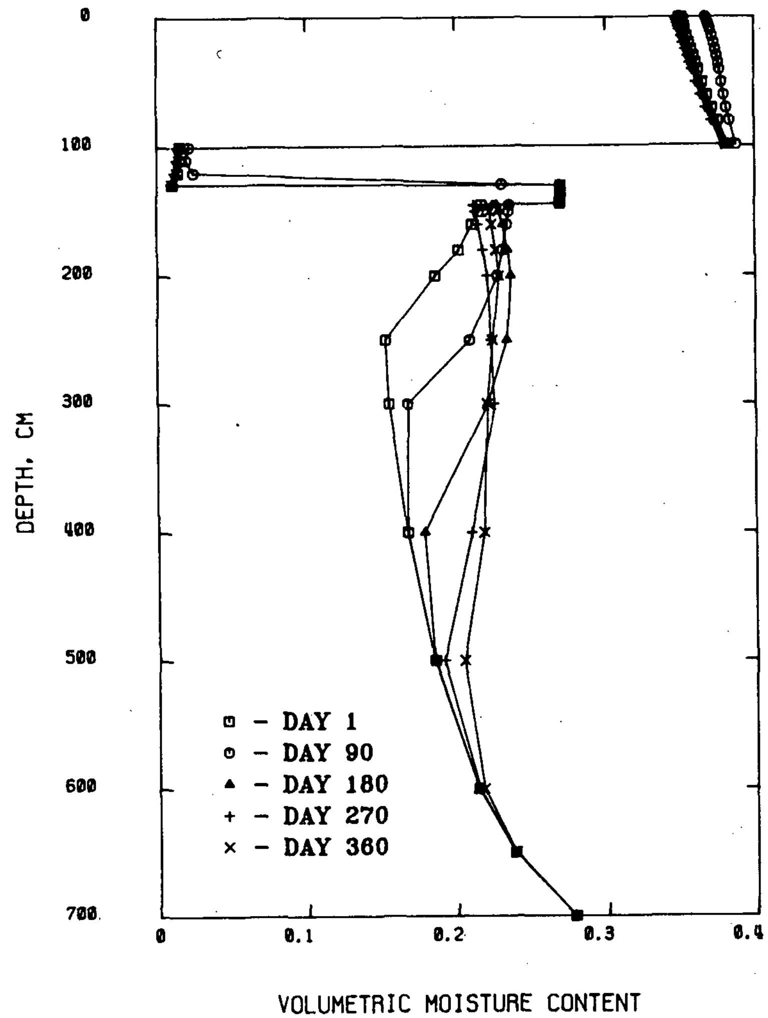

FIGURE 6a. Moisture Content Distribution for Rock Cover, Wet Year (1979) Climate Data --2nd Simulation Year

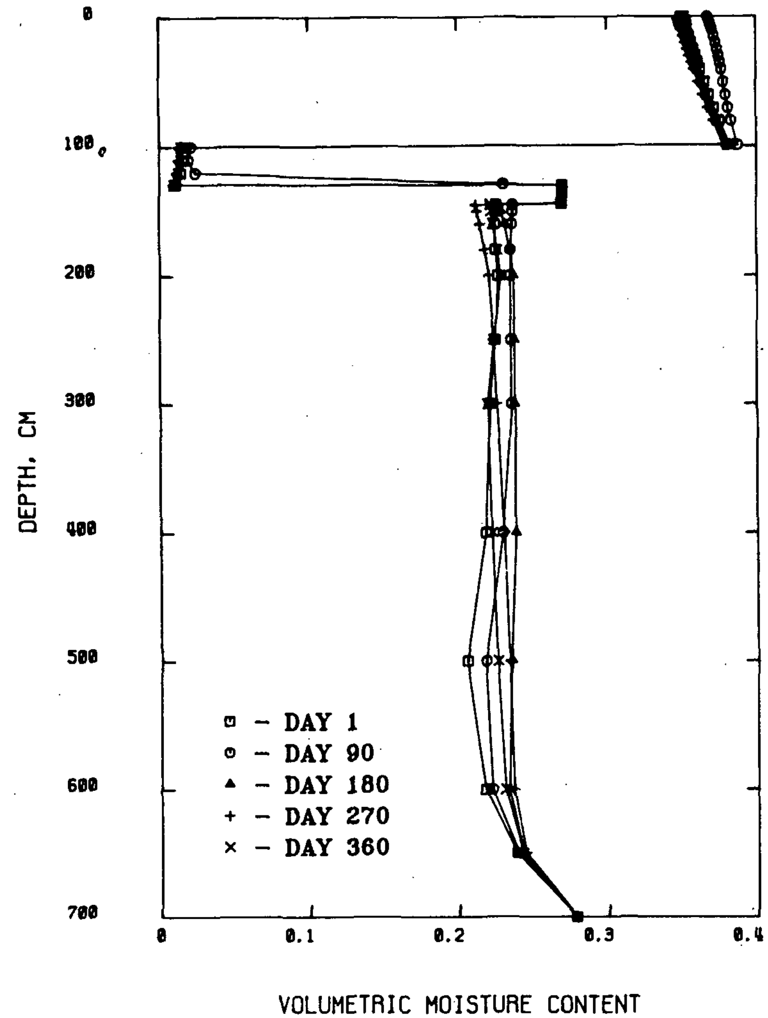

FIGURE 6b. Moisture Content Distribution for Rock Cover, Wet Year (1979) Climate Data--3rd Simulation Year

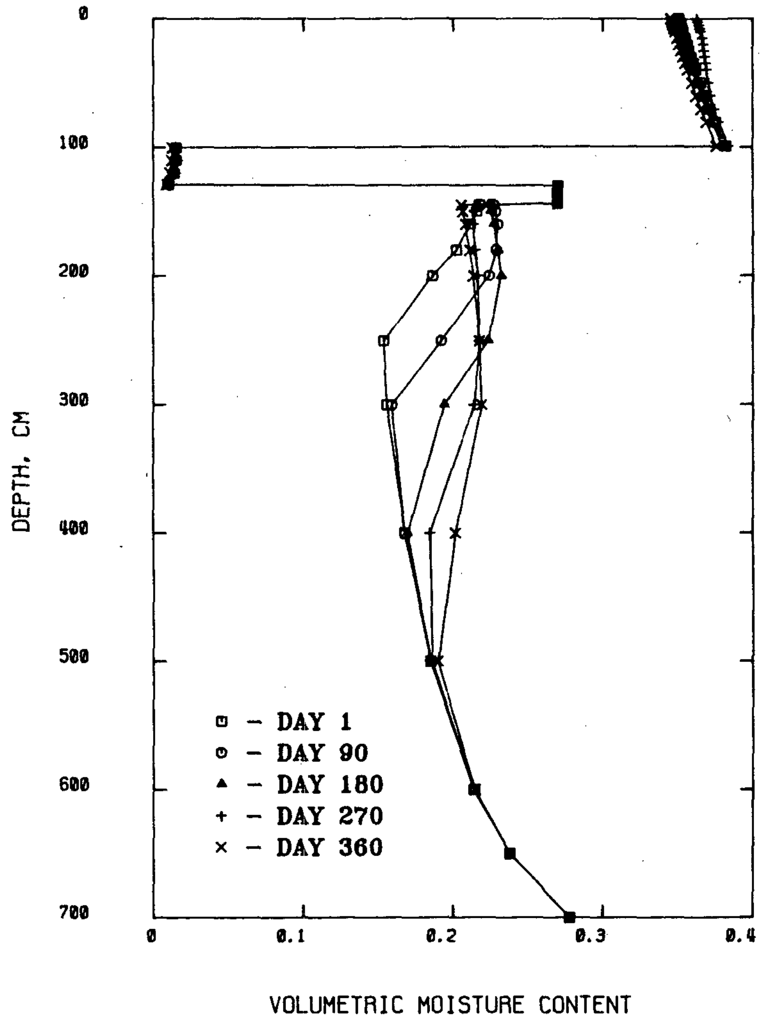

FIGURE 7a. Moisture Content Distribution for Rock Cover, Dry Year (1976) Climate Data --2nd Simulation Year

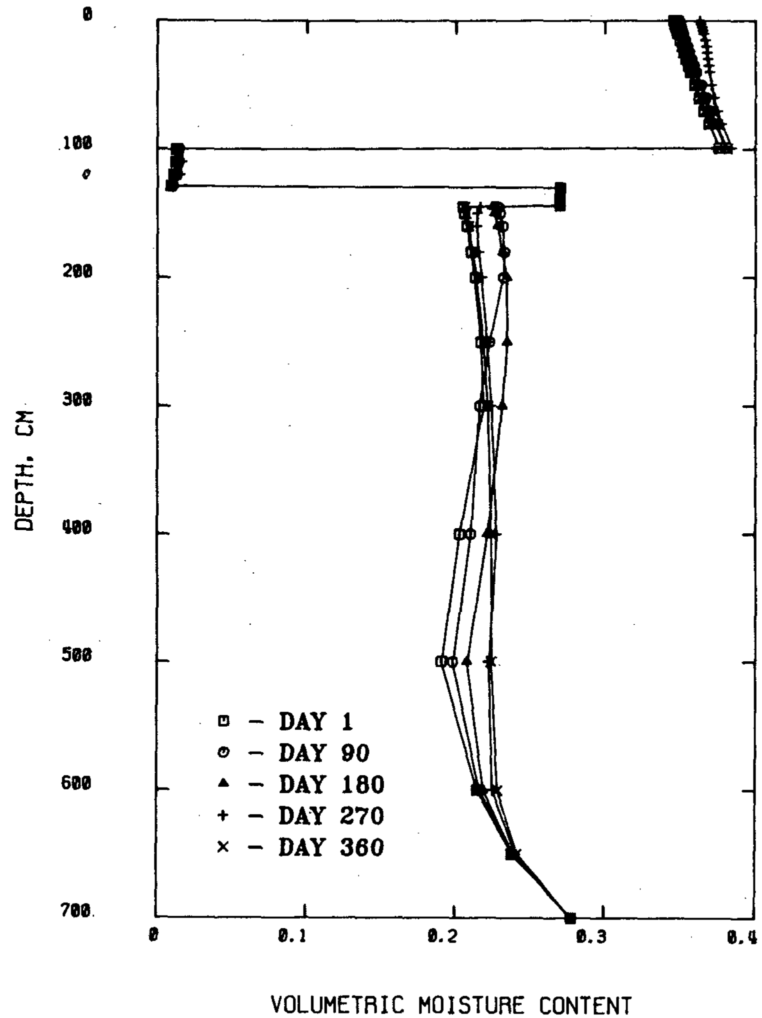

FIGURE 7b. Moisture Content Distribution for Rock Cover, Dry Year (1976) Climate Data--3rd Simulation Year

The moisture storage in the tailings pile is shown in Figures 8a and 8b and in Figures 9a and 9b. These results indicate a significant increase in the moisture storage. For the wet year case, the moisture storage increases until the middle of the third year, at which point a decrease and subsequent leveling out occurs. This probably occurs because the drainage from the soil profile is starting to balance the moisture input. A similar trend is observed for the dry year case, although the moisture storage is not as great.

Tables 6 and 7 summarize the water balance for the wet and dry years, respectively. It is apparent that the rock cover has caused a significant increase in the moisture storage relative to vegetation. This increase arises because the evaporation from the rock cover is significantly lower than for the vegetated cover. The moisture loss from the combined runoff and evaporation for the rock cover is on the order of 1 cm of water per year. The moisture loss due to evapotranspiration from the vegetated cover is between 10 and 20 cm of water per year. This means that the moisture input to a tailings pile with a rock cover in a setting similar to that at Grand Junction, Colorado exceeds the moisture input with a vegetated cover by more than 10 cm of water. Significantly, the moisture input for the rock cover case exceeds the ability of the soil profile to store water; hence, drainage from the system occurs.

The evaporation model that has been used for the rock cover is simplistic, but even a two- or three-fold increase in surface evaporation would not change these qualitative results.

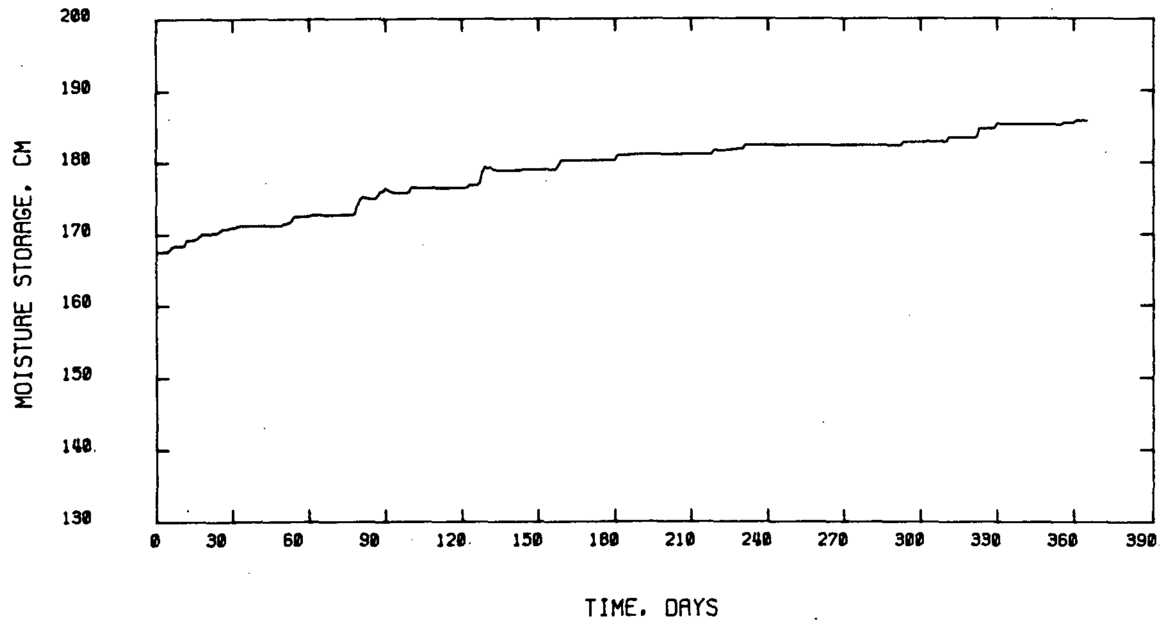

FIGURE 8a. Moisture Storage with Rock Cover, Wet Year (1979) Climate Data--2nd Simulation Year

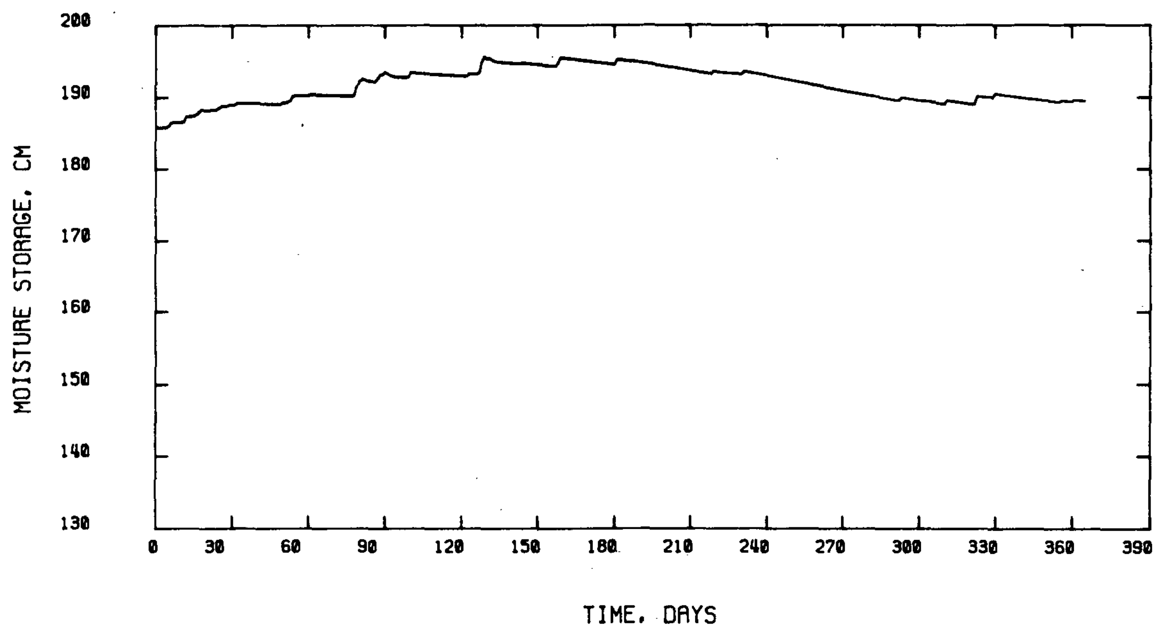

FIGURE 8b. Moisture Storage with Rock Cover, Wet Year (1979) Climate Data--3rd Simulation Year

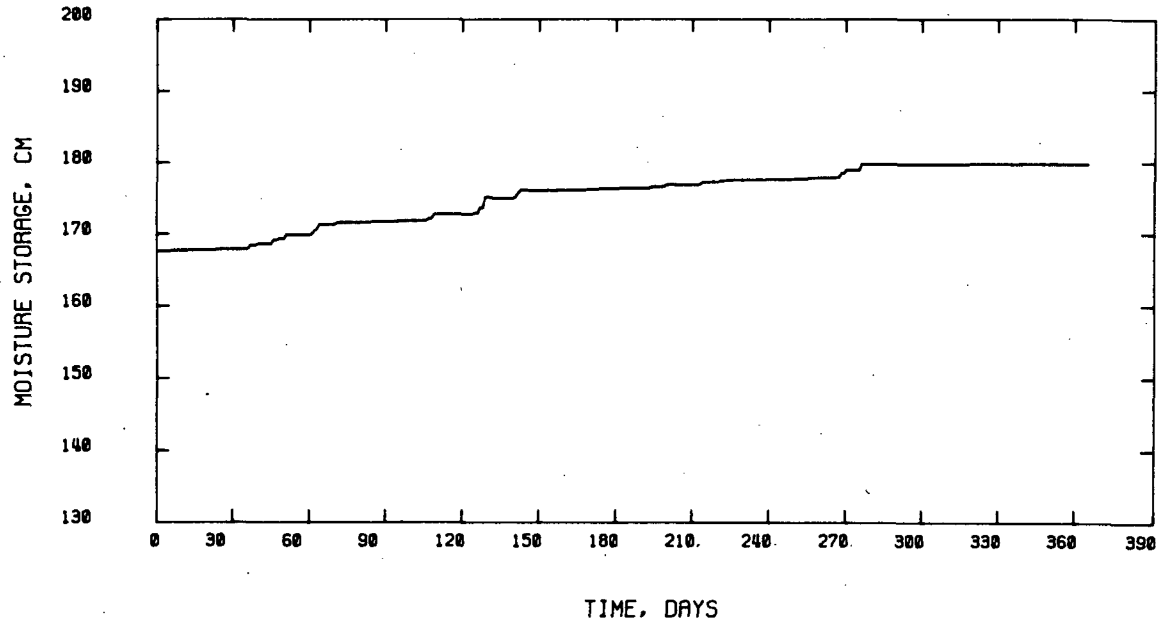

FIGURE 9a. Moisture Storage with Rock Cover, Dry Year (1976) Climate Data--2nd Simulation Year

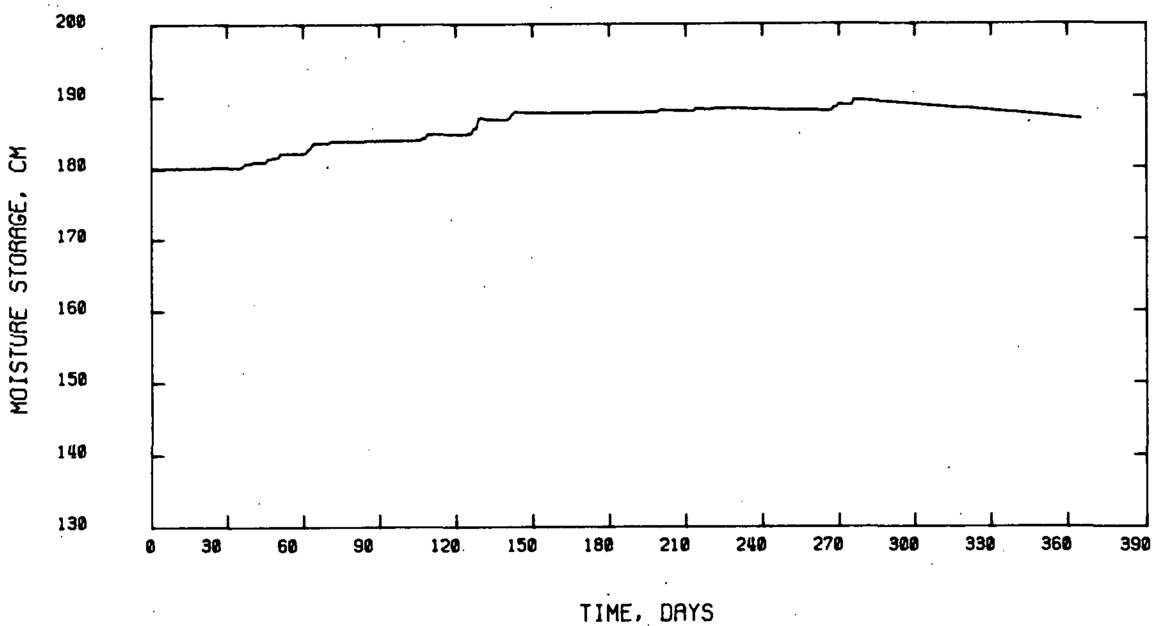

FIGURE 9b. Moisture Storage with Rock Cover, Dry Year (1976) Climate Data--3rd Simulation Year

TABLE 6. Water Balance for Two Wet Years, Rock Cover System

Water (cm)	Simulation Year	
	2	3
Initial Storage	167.5	185.8
Rainfall	22.6	22.6
Runoff	0.8	0.8
Evaporation	0.2	0.2
Transpiration	0.0	0.0
Drainage	0.4	15.1
Final Storage	185.8	189.4
Mass Balance Error	2.8	2.8

TABLE 7. Water Balance for Two Dry Years, Rock Cover System

Water (cm)	Simulation Year	
	2	3
Initial Storage	167.5	179.9
Rainfall	13.4	13.4
Runoff	0.4	0.4
Evaporation	0.2	0.2
Transpiration	0.0	0.0
Drainage	0.1	5.4
Final Storage	179.9	186.8
Mass Balance Error	0.4	0.4

REFERENCES

Branson, R. A., R. F. Miller and I. S. McQueen. 1970. "Plant Communities and Associated Soil and Water Factors on Shale-Derived Soils in Northeastern Montana." Ecology, Vol. 51, No. 3, pp. 391-407.

Branson, F. A., R. F. Miller and I. S. McQueen. 1976. "Moisture Relationships in Twelve Northern Desert Shrub Communities Near Grand Junction, Colorado." Ecology, Vol. 57, pp. 1104-1124.

Cline, J. F., and W. H. Rickard. 1974. "Belowground Plant Biomass in the Shrub-Steppe Ecosystem." In: Pacific Northwest Laboratory Annual Report of 1973. Vol. 1, Part 2, pp. 161-162. BNWL-1850, Pacific Northwest Laboratory, Richland, Washington.

Gupta, S. K., K. K. Tanji, D. R. Nielsen, J. W. Biggar, C. S. Simmons and J. L. MacIntyre. 1978. Field Simulation of Soil-Water Movement with Crop Water Extraction. Water Science and Engineering Papers No. 4013, Department of Land, Air, and Water Resources, University of California, Davis, California.

Mayer, D. W., C. A. Oster, R. W. Nelson and G. W. Gee. 1981. Radon Diffusion Through Multilayer Earthen Covers: Models and Simulations. PNL-3989, Pacific Northwest Laboratory, Richland, Washington.

Nelson, R. W., G. W. Gee and C. A. Oster. 1980. "Radon Control by Multilayer Earth Barriers, 1. Modeling of Moisture and Density Effects on Radon Diffusion from Uranium Mill Tailings." In: Uranium Mill Tailings Management, Proceedings of the Third Symposium, November 24-25, 1980, pp. 79-88. Geotechnical Engineering Program, Civil Engineering Department, Colorado State University.

Simmons, C. S., and G. W. Gee. 1981. Simulation of Water Flow and Retention in Cover Materials Overlaying Uranium Mill Tailings. PNL-3877, Pacific Northwest Laboratory, Richland, Washington.

APPENDIX

ROOT DENSITY FUNCTIONS

APPENDIX

ROOT DENSITY FUNCTIONS

The root density function, r(z), is a probability curve that predicts the fraction of the total plant root existing at a given depth. For this study, a step function has been used instead of a smooth curve. Tables A.1 through A.4 tabulate the density function used for each of the plant species. Tables A.1 and A.2 are based on data reported by Branson et al. 1976. Tables A.3 and A.4 are based on data reported by Cline and Rickard 1974. The composite density function used to simulate the composite plant community was calculated by summing the root density function for each plant using appropriate weighting factors. The composite root density is then used to determine the rate at which moisture is extracted by the plants at various depths.

TABLE A.1. Root Density Function for *Artemisia tridentata*

Depth Interval, cm	Normalized Depth Interval, z/z_{max}	Root Weights, g/dm^3	r(z) 1/cm
0-10	0 - 0.0556	287.2	0.01854
10-20	0.0556 - 0.1111	243.1	0.01570
20-30	0.1111 - 0.1667	251.3	0.01623
30-40	0.1667 - 0.2222	143.6	0.00927
40-50	0.2222 - 0.2778	105.6	0.00682
50-60	0.2778 - 0.3333	92.3	0.00596
60-70	0.3333 - 0.3889	95.4	0.00616
70-80	0.3889 - 0.4444	25.6	0.00165
80-90	0.4444 - 0.5000	20.5	0.00132
90-100	0.5000 - 0.5556	30.8	0.00199
100-110	0.5556 - 0.6111	33.8	0.00218
110-120	0.6111 - 0.6667	25.6	0.00165
120-130	0.6667 - 0.7222	20.5	0.00132
130-140	0.7222 - 0.7778	44.1	0.00285
140-150	0.7778 - 0.8333	44.1	0.00285
150-160	0.8333 - 0.8889	30.8	0.00199
160-170	0.8889 - 0.9444	30.8	0.00199
170-180	0.9444 - 1.0000	23.6	0.00152
	Total	1548.7	

TABLE A.2. Root Density Function for *Atriplex confertifolia*

Depth Interval, cm	Normalized Depth Interval, z/z_{max}	Root Weights, g/m^2	r(z) 1/cm
0-10	0 - 0.0909	70.5	0.01587
10-20	0.0909 - 0.1818	57.9	0.01303
20-30	0.1818 - 0.2727	52.6	0.01184
30-40	0.2727 - 0.3636	42.1	0.00948
40-50	0.3636 - 0.4545	47.4	0.01067
50-60	0.4545 - 0.5455	31.6	0.00711
60-70	0.5455 - 0.6364	45.3	0.01020
70-80	0.6364 - 0.7273	28.4	0.00639
80-90	0.7273 - 0.8182	26.3	0.00592
90-100	0.8182 - 0.9091	24.2	0.00545
100-110	0.9091 - 1.0000	17.9	0.00403
	Total	444.2	

TABLE A.3. Root Density Function for *Agropyron*

Depth Interval, cm	Normalized Depth Interval, z/z_{max}	Root Weights, g/m^2	r(z) 1/cm
0-10	0 - 0.125	348	0.02924
10-20	0.125 - 0.25	196	0.01647
20-30	0.25 - 0.375	144	0.01210
30-40	0.375 - 0.5	120	0.01008
40-50	0.5 - 0.625	118	0.00992
50-60	0.625 - 0.75	108	0.00908
60-70	0.75 - 0.875	98	0.00824
70-80	0.875 - 1.0	58	0.00487
	Total	1190	

TABLE A.4. Root Density Function for *Bromus tectorum*

Depth Interval, cm	Normalized Depth Interval, z/z_{max}	Root Weights, g/m^2	r(z) 1/cm
0-10	0 - 0.125	499.4	0.06302
10-20	0.125 - 0.250	145.5	0.01836
20-30	0.250 - 0.375	51.1	0.00645
30-40	0.375 - 0.500	31.5*	0.00398
40-50	0.500 - 0.625	25.6	0.00323
50-60	0.625 - 0.750	15.7	0.00198
60-70	0.750 - 0.875	11.8	0.00149
70-80	0.875 - 1.000	11.8	0.00149
	Total	792.4	

* Interpolated from published data.

DISTRIBUTION

No. of Copies

OFFSITE

A. A. Churm
DOE Chicago Patent Group
9800 South Cass Avenue
Argonne, IL 60439

27 DOE Technical Information Center

R. E. Cunningham
Office of Nuclear Safety
Materials and Safeguards
Room 562
Nuclear Regulatory Commission
7915 Eastern Avenue
Silver Springs, MD 20910

Waste Management Research Branch
Division of Safeguards
Fuel Cycle and Environmental Research
Nuclear Regulatory Commission
Washington, DC 20545

P. E. Leader
New Uranium Mill Licensing Section
Nuclear Regulatory Commission
Washington, DC 20545

H. J. Miller
New Uranium Mill Licensing Section
Nuclear Regulatory Commission
Washington, DC 20545

W. E. Mott
DOE Division of Environmental Control Technology
Washington, DC 20545

No. of Copies

R. A. Scarano, Chief
Uranium Recovery License Branch
U.S. Nuclear Regulatory Commission
Mail Station 483-SS
Washington, DC 20555

S. A. Mann
DOE Chicago Operations and Region Office
Argonne, IL 60439

J. O. Neff
DOE Columbus Program Office
505 King Avenue
Columbus, OH 43201

J. P. Hamric
DOE Idaho Operations Office
505 King Avenue
Idaho Falls, ID 83401

2 J. B. Whitsett
DOE Idaho Operations Office
505 King Avenue
Idaho Falls, ID 83401

S. W. Ahrends
DOE Oak Ridge Operations Office
P. O. Box E
Oak Ridge, TN 37380

L. Keller
DOE Oak Ridge Operations Office
P. O. Box E
Oak Ridge, TN 37380

D. E. Large
DOE Oak Ridge Operations Office
P. O. Box E
Oak Ridge, TN 37380

Beverly Rawles
Office of Nuclear Waste Isolation
505 King Avenue
Columbus, OH 43201

No. of
Copies

T. B. Hindman
DOE Savannah River Operations Office
P. O. Box A
Aiken, SC 29801

R. P. Whitfield
DOE Savannah River Operations Office
P. O. Box A
Aiken, SC 29801

W. B. Wilson
DOE Savannah River Operations Office
P. O. Box A
Aiken, SC 29801

S. G. Harbinson
DOE San Francisco Operations Office
1333 Broadway
Oakland, CA 94612

S. Lichtman
Criteria and Standards Division
Office of Radiation Programs
Environmental Protection Agency
Washington, DC 20460

Environmental Protection Agency
Technological Assessment Division (AW-559)
Office of Radiation Programs
Washington, DC 20460

J. G. Themelis, Director
Engineering and Safety Division
DOE Grand Junction Office
P. O. Box 2567
Grand Junction, CO 81501

Robert Williams
Electric Power Research Institute
3412 Hillview Avenue
Palo Alto, CA 94304

No. of
Copies

4 T. Gerusky, Director
Bureau of Radiation Protection
P. O. Box 2063
Harrisburg, PA 17120

4 Edgar D. Bailey
P. E., Administrator
Radiation Control Branch
Texas Department of Health
1100 W. 49th Street
Austin, TX 78756

4 A. J. Hazle, Director
Radiation and Hazardous Wastes Division
Colorado Department of Health
4210 East 11th Avenue
Denver, CO 80220

4 Ted Wolfe, Environmental Manager
Radiation Department
P. O. Box 968
Santa Fe, NM 87503

4 Lynn Frank, Director
Oregon Department of Energy
111 Labor and Industries Building
Salem, OR 97310

4 Dana K. Mount
P. E., Director
Division of Environmental Engr.
North Dakota State Department of Health
1200 Missouri Avenue
Room 304
Bismark, ND 58505

4 Robert Funderberg
Department of Health and Welfare
Statehouse
Boise, ID 83707

4 Harold Tso, Executive Director
Environmental Protection Commission
Navajo Tribe
Window Rock, AZ 86515

No. of
Copies

4 John W. McKiernan
Organization 4542
Sandia National Laboratory
P. O. Box 5800
Albuquerque, NM 87185

Gergely Markos,
Uranium Research Program
GEC Research, Inc.
2693 Commerce Road
Rapid City, SD 57701

Vern C. Rogers
P. E., President
Rogers and Associates Engineering
445 East 200 South, Suite 303
Salt Lake City, UT 84111

4 Larry Anderson, Director
Bureau of Radiation and
Occupational Health
P. O. Box 2500
Salt Lake City, UT 84110

W. Nixon
Office of Nuclear Materials Safety
and Safeguards
U.S. Regulatory Commission
Mail Station 396-SS
Washington, DC 20555

G. Birchard
U.S. Nuclear Regulatory Commission
Mail Station 1130-SS
Washington, DC 20555

W. M. Shaffer
Uranium Recovery Licensing Branch
U.S. Nuclear Regulatory Commission
Mail Station 461-SS
Washington, DC 20555

A. Topp, Chief
Radiation Protection Bureau
P. O. Box 968
Santa Fe, NM 87503

No. of
Copies

4 Walt Ackerman, Director
Department of Environmental
Quality
Land Quality Division
Hathaway Building
Cheyenne, WY 82002

Lynn Fitzrondolph
Arizona Atomic Energy Commission
2929 West Indian School Road
Phoenix, AZ 85017

Robert Overmyer
Ford, Bacon and Davis-Utah
P. O. Box 8009
Salt Lake City, UT 84108

W. Chappell
University of Colorado-Denver
P. O. Box 136
Denver, CO 80202

D. Dressen
Los Alamos Scientific Laboratory
P. O. Box 1663
Los Alamos, NM 87545

W. Kislieski
Argonne National Laboratory
9700 South Cass Avenue
Argonne, IL 60439

John D. Nelson
Colorado State University
Ft. Collins, CO 80523

R. Kennedy
Ford, Bacon and Davis-Utah
Utah Operations
2009 N. 14th Street
Suite 603
Arlington, VA 20009

F. Haywood
Oak Ridge National Laboratory
P. O. Box X
Oak Ridge, TN 37830

No. of Copies

A. Ryon
Oak Ridge National Laboratory
P. O. Box X
Oak Ridge, TN 37830

W. Staub
Oak Ridge National Laboratory
P. O. Box X
Oak Ridge, TN 37830

T. Tamura
Oak Ridge National Laboratory
P. O. Box X
Oak Ridge, TN 37830

J. Morse
Colorado Energy Research Institute
2221 East Street
Golden, CO 80401

R. Olson
Civil Engineering Department
University of Texas
Crockrell Hall
Austin, TX 78712

Al Askew
Politech Corporation
2220 Austin National Bank Tower
Austin, TX 78701

J. N. Dybalski
Armak Company
8401 W. 47th Street
McCook, IL 60525

D. H. Groelsema
U.S. Department of Energy
NE 301
Mail Station B-107
Washington, DC 20545

E. Delaney
U.S. Department of Energy
NE 301
Mail Station B-107
Washington, DC 20545

No. of Copies

W. W. Ballard
U.S. Department of Energy
NE 301
Mail Station B-107
Washington, DC 20545

M. G. White
U.S. Department of Energy
NE 301
Mail Station B-107
Washington, DC 20545

K. Baker
U.S. Department of Energy
NE 20
Mail Station B-107
Washington, DC 20545

S. Meyers
U.S. Department of Energy
NE 30
Mail Station B-107
Washington, DC 20545

R. Ramsey
U.S. Department of Energy
NE 30
Mail Station B-107
Washington, DC 20545

G. Oertel
U.S. Department of Energy
NE 320
Mail Station B-107
Washington, DC 20545

A. Kluk
U.S. Department of Energy
NE 320
Mail Station B-107
Washington, DC 20545

R. Romatowski
U.S. Department of Energy
Albuquerque Operations Office
P.O. Box 5400
Albuqurque, NM 87185

No. of Copies	
	R. Y. Lowery U.S. Department of Energy Albuquerque Operations Office P.O. Box 5400 Albuqurque, NM 87185
	R. H. Campbell U.S. Department of Energy Albuquerque Operations Office P.O. Box 5400 Albuqurque, NM 87185
	M. L. Matthews U.S. Department of Energy Albuquerque Operations Office P.O. Box 5400 Albuqurque, NM 87185
	T. N. Narasimhan Lawrence Berkeley Laboratory Earth Sciences Division University of California Berkeley, CA 94720

ONSITE

2	DOE Richland Operations Office H. E. Ransom J. D. White
4	Rockwell Hanford Operations J. D. Roecker D. D. Wodrich (3)
	UNC United Nuclear Industries F. H. Bouse

No. of Copies	
	Westinghouse Hanford Company A. G. Blasewitz
61	Pacific Northwest Laboratory S. M. Barnes P. A. Beedlow (10) W. F. Bonner C. A. Brown S. M. Brown J. L. Buelt L. L. Cadwell D. B. Cearlock T. D. Chikalla J. F. Cline M. R. Elmore H. D. Freeman G. W. Gee V. Q. Hale J. N. Hartley P. L. Koehmstedt J. M. Latkovich G. B. Long (3) D. W. Mayer (10) J. L. McElroy M. C. McShane J. Mishima D. A. Nelson R. W. Nelson B. Opitz A. M. Platt L. C. Schwendiman D. Sherwood D. J. Silviera C. S. Simmons P. C. Walkup/R. E. Nightingale M. L. Warner B. E. Vaughan J. Zellmer Technical Information (5) Publishing Coordination BE (2)